

High-cycle fatigue tests of pretensioned concrete beams

Jörn Remitz and Martin Empelmann

- This paper compares the predicted fatigue life of prestressed concrete beams based on experimental data with currently accepted design methods and specifications.
- The experimental data came from a literature review of previous studies as well as experimental testing of nine beams for this study, which included multiple concrete and tensile reinforcement configurations.
- The study found that current models for predicting fatigue life overestimate the fatigue life of embedded strands in pretensioned concrete beams, especially at low stress ranges.

Precast, pretensioned concrete beams are often used as bridge girders for simply supported bridges. Because these girders are repeatedly subjected to loads caused by high and heavy traffic, fatigue resistance is an important part of their design. In general, the fatigue resistance of pretensioned concrete beams under cyclic loading is influenced mainly by the fatigue of the embedded prestressing steel. In current specifications and standards, the fatigue verification of prestressing steel is either based on S-N curves, which describe the relationship between the steel stress range and the fatigue life (number of load cycles to failure), or on a fatigue endurance limit. For example, the European Committee for Standardization's *Eurocode 2*¹ (EC2) and the *fib* (International Federation for Structural Concrete) *fib Model Code for Concrete Structures 2010*² (MC2010) use S-N curves and the American Association of State Highway and Transportation Officials' *AASHTO LRFD Bridge Design Specifications*³ and The American Concrete Institute's *Considerations for the Design of Concrete Structures Subjected to Fatigue Loading*⁴ (ACI PRC-215) use fatigue endurance limits. To evaluate the flexural fatigue behavior of pretensioned concrete beams, international fatigue test results of pretensioned concrete beams under cyclic bending loads were summarized in a database and analyzed with regard to fatigue resistance.

Various authors have conducted flexural fatigue tests on pretensioned concrete beams with straight bonded strands or wires.⁵⁻²¹ For example, Empelmann and Sender²² and Maurer et al.²³ summarize detailed data of previous fatigue tests and results. The test results shown in **Fig. 1** suggest that the fatigue

PCI Journal (ISSN 0887-9672) V. 67, No. 1, January–February 2022.

PCI Journal is published bimonthly by the Precast/Prestressed Concrete Institute, 8770 W. Bryn Mawr Ave., Suite 1150, Chicago, IL 60631.

Copyright © 2022, Precast/Prestressed Concrete Institute. The Precast/Prestressed Concrete Institute is not responsible for statements made by authors of papers in *PCI Journal*. Original manuscripts and discussion on published papers are accepted on review in accordance with the Precast/Prestressed Concrete Institute's peer-review process. No payment is offered.

failure mode of such beams depends on the maximum fatigue load level FLL_{max} , which is defined as the ratio of the maximum fatigue load or moment $M_{fat,max}$ and the ultimate capacity M_u :

$$FLL_{max} = M_{fat,max} / M_u$$

Maximum fatigue load levels greater than about 70% of ultimate capacity usually result in concrete compression failure of pretensioned concrete beams. Fatigue load levels less than about 70% mainly cause failure of the prestressing steel.

Concrete compression failure:

$$FLL_{max} \geq 0.70$$

Prestressing steel failure:

$$FLL_{max} < 0.70$$

Because load levels in bridges are usually below this value, the fatigue behavior of prestressing steel is considered to be critical to the fatigue life of pretensioned concrete beams.

Figure 2 shows the fatigue test results of beams that failed by fatigue of the prestressing steel in relation to the steel stress range. The results are compared with test results of single strands in air under cyclic tension from Paulson et al.²⁴ as well as with the S-N curve for pretensioned steel according to EC2 and MC2010 and the fatigue endurance limit according to AASHTO LRFD specifications and ACI PRC-215 (assuming a tensile strength for the strands of 1770 MPa [257 ksi, approximately Grade 250]). While the normative S-N curve according to EC2 and MC2010 can be assumed as a lower-bound approach for the fatigue life of single strands in air, the S-N curve does not properly reflect the test results of strands in pretensioned concrete beams. Even though single strands and embedded

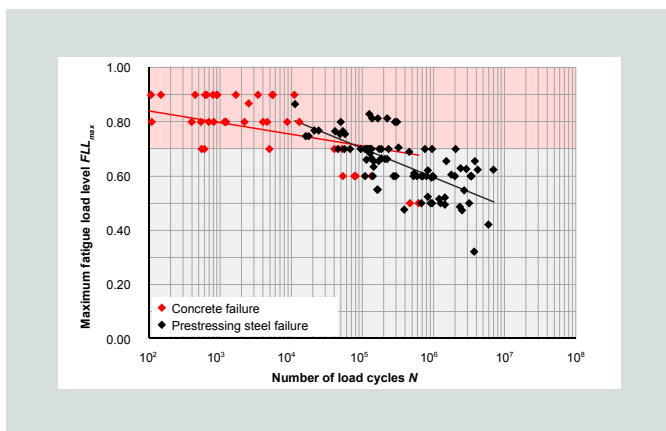


Figure 1. Fatigue test results of pretensioned concrete beams based on the fatigue load level. Note: Concrete failure = results from Venuti (1965) and Slepetz (1968); Prestressing steel failure = results from Ozell and Ardaman (1956); Nordby and Venuti (1957); Bate (1962); Warner and Hulsbos (1964); Venuti (1965); Abeles, Brown, and Hu (1974); Rabbat, Kaar, Russel, and Bruce (1979); Harajli and Naaman (1984); Overman, Breen, and Frank (1984); Muller and Dux (1992); and Rao and Frantz (1996).

strands in beams have a similar fatigue life at stress ranges $\Delta\sigma_p$ greater than approximately 200 MPa (29 ksi), the fatigue life of strands in beams is, in many cases, significantly lower than that of single strands at stress ranges $\Delta\sigma_p$ less than 200 MPa and thus lower than the fatigue life according to the normative S-N curve. This reduced fatigue life of embedded strands can be explained by the structural parameters of pretensioned concrete beams (for example, reinforcing and prestressing steel ratio) as well as specific fatigue processes (for example, fretting effects caused by cyclic friction between strands and concrete) (**Fig. 3**), which have been investigated and discussed in detail in previous publications.^{14,25-27} These influences affect fatigue behavior especially at low stress ranges. Moreover, some tests had prestressed concrete beams that failed well below the endurance limit according to the AASHTO LRFD specifications and ACI PRC-215. To check the high-cycle fatigue of embedded strands in pretensioned concrete beams, this study conducted additional fatigue tests with steel stress ranges of about 100 MPa (14.5 ksi) and load cycles between 10^6 and 10^8 .

Experimental investigation

Test specimens

A total of nine I-beams with a length of 5.00 m (16.4 ft) and a height of 0.50 m (1.64 ft) were tested with strand stress ranges of about 100 MPa (14.5 ksi) and varying concretes and tensile reinforcements as the main structural parameters. All beams were dimensioned to generate flexural fatigue failure caused by fatigue of the embedded strands. **Figure 4** and **Table 1** show the dimensions and structural parameters of the test beams. The first test (beam B5) was conducted during a previous research project.²⁸ The other eight beams were produced simultaneously in pairs (B6 and B7, B8 and B9, B10 and B11, and B12 and B13). The beams were made of either normal-strength C50/60 concrete or high-strength C80/95 concrete. Based on concrete

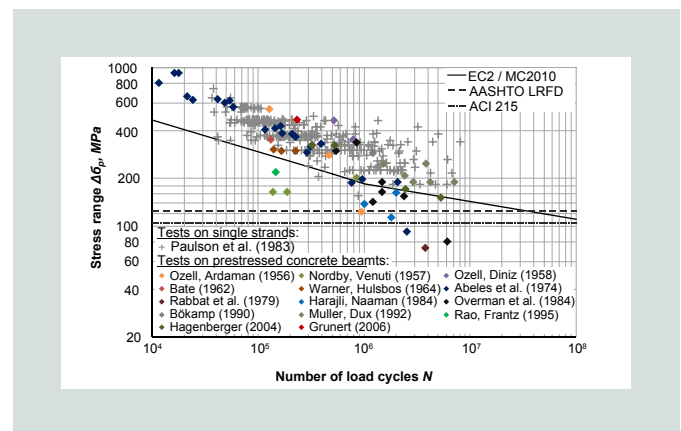


Figure 2. Fatigue test results of pretensioned concrete beams based on the stress range in prestressing steel. Note: AASHTO LRFD = American Association of State Highway and Transportation Officials' *AASHTO LRFD Bridge Design Specifications*; ACI 215 = the American Concrete Institute's *Considerations for the Design of Concrete Structures Subjected to Fatigue Loading* (ACI PRC-215-92); EC2/MC2010 = European Committee for Standardization's *Eurocode 2 or fib Model Code for Concrete Structures* 2010. 1 MPa = 0.145 ksi.

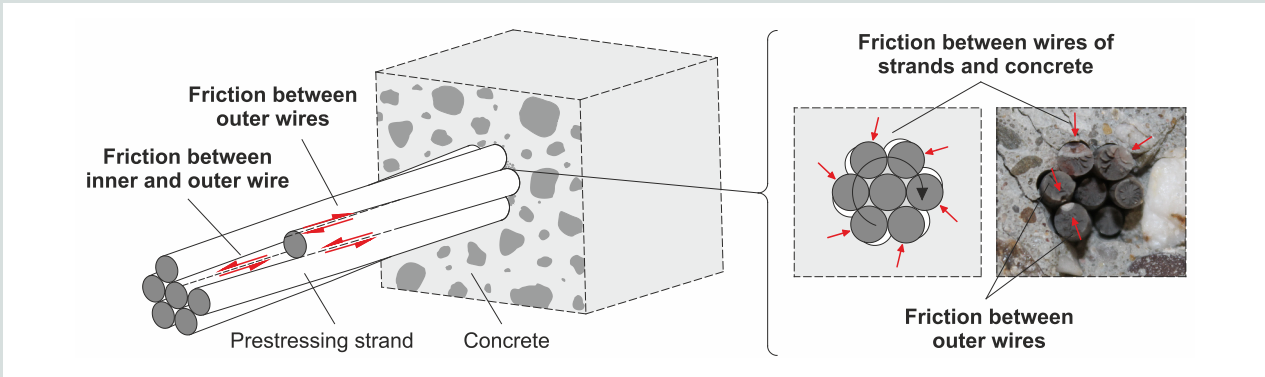


Figure 3. Friction processes at strands in concrete and resulting wire breaks. Source: Remitz and Empelmann (2020).

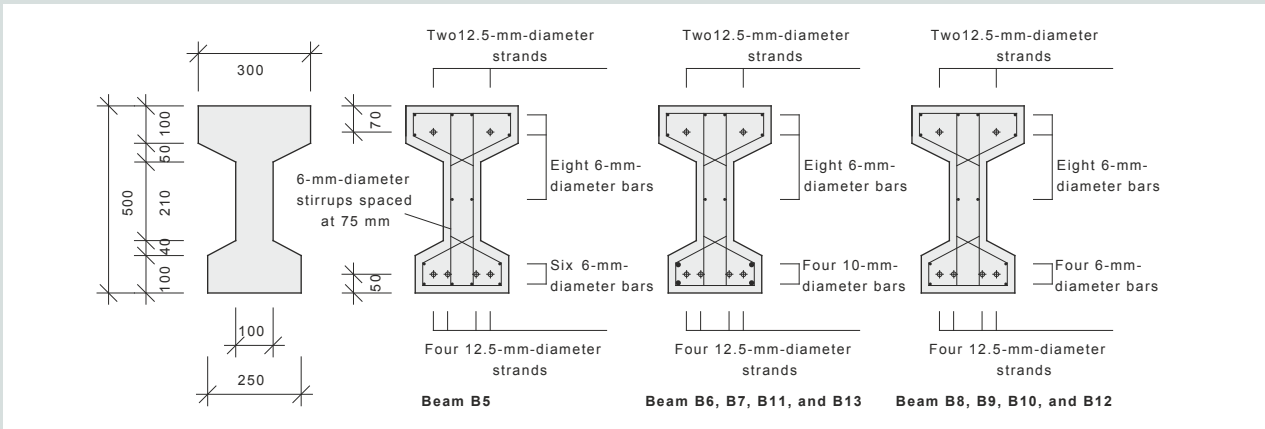


Figure 4. Cross section and reinforcement of the beams and pictures of beam production. Note: All dimensions are in millimeters. 1 mm = 0.0394 in.

cylinder testing at the beginning of the fatigue tests, the stress-strain relationship of the normal- and high-strength concretes was determined including average values of the compressive strength $f_{cm,cyl}$, splitting tensile strength $f_{cm,sp}$, and modulus of elasticity E_{cm} (Table 1). Furthermore, the amount of Grade B500 tensile reinforcement (minimum tensile strength of 500 MPa [72 ksi]) was varied, with some beams using four 6 mm (0.24 in.) diameter reinforcing bars with a total area of reinforcing steel A_s equal to 113 mm² (0.175 in.²) and other beams using four 10 mm (0.39 in.) diameter reinforcing bars with

A_s equal to 314 mm² (0.487 in.²). The average yield strength, tensile strength, and modulus of elasticity of the reinforcement was determined using tensile tests to be about 555, 600, and 200,000 MPa (80.5, 87.0 and 29,000 ksi), respectively. In all beams, four Grade St1660/1860 seven-wire strands (minimum tensile strength of 1860 MPa [270 ksi]) with a diameter of 12.5 mm (0.5 in.) and an area of prestressing strands A_p of 93 mm² (0.144 in.²) were used in the tensile zone for a total A_p of 372 mm² (0.577 in.²). Two additional strands were arranged in the top flange to prevent cracking after prestressing. The strands

Table 1. Structural parameters of beams

Beam	Concrete					Tensile reinforcement	Pre-stressing strands	Prestressing	
	Class	Age, days	Average concrete compressive strength $f_{cm,cyl}^a$ MPa	Average concrete splitting tensile strength $f_{ctm,sp}^a$ MPa	Average concrete modulus of elasticity E_{cm}^a MPa			Initial prestressing steel/strand stress $\sigma_p^{(0)}$, MPa	Prestressing steel/strand stress at start of test $\sigma_{p,t}^b$ MPa
B5*	C80/95	28	102.8	5.0	43,200	Six 6 mm diameter bars	Four 12.5 mm diameter strands	1080	965
B6	C50/60	135	71.0	4.5	36,000	Four 10 mm diameter bars	Four 12.5 mm diameter strands	1100	896
B7	C50/60	218	71.1	4.8	37,800	Four 10 mm diameter bars	Four 12.5 mm diameter strands	1100	887
B8	C80/95	28	87.3	3.9	41,800	Four 6 mm diameter bars	Four 12.5 mm diameter strands	1100	974
B9.1	C80/95	56	92.4	4.0	41,100	Four 6 mm diameter bars	Four 12.5 mm diameter strands	1100	953
B9.2	C80/95	56	92.4	4.0	41,100	Four 6 mm diameter bars	Four 12.5 mm diameter strands	1100	953
B10	C80/95	148	90.0	5.1	45,800	Four 6 mm diameter bars	Four 12.5 mm diameter strands	1100	930
B11	C80/95	118	88.4	4.8	44,500	Four 10 mm diameter bars	Four 12.5 mm diameter strands	1100	935
B12	C50/60	28	59.5	4.3	32,900	Four 6 mm diameter bars	Four 12.5 mm diameter strands	1100	935
B13	C50/60	97	69.3	4.3	38,300	Four 10 mm diameter bars	Four 12.5 mm diameter strands	1100	914

Note: 1 MPa = 0.145 ksi; 1 mm = 0.0394 in.

* Beam B5 was tested during a previous research project (Remitz and Empelmann [2015]).

had an average 0.1% yield strength of 1710 MPa (248 ksi), tensile strength of 1920 MPa (278 ksi), and modulus of elasticity of 198,000 MPa (28,700 ksi).

Beams B6 and B12, constructed with C50/60 concrete, as well as beams B8 and B11, constructed with C80/95 concrete, differed only in the amount of tensile reinforcing steel and were tested with a similar stress range $\Delta\sigma_p$ of about 100 MPa [14.5 ksi]. Based on these tests, the influence of varying amounts of reinforcement was investigated. In addition, beams B6 and B11, as well as beams B8 and B12, which had the same reinforcement, were used to examine the influence of different types of concrete. Beam B7, with the same configuration as beam B6, was periodically loaded to an overload of 120% of the upper cyclic load level to explore the influence of overloads. Beams B9, B10, and B13 were tested at strand stress ranges less than 100 MPa to check a possible endurance limit. Beam B9 withstood the anticipated number of load cycles with no indication of failure (B9.1), so the test was stopped and continued at an increased cyclic load level (B9.2).

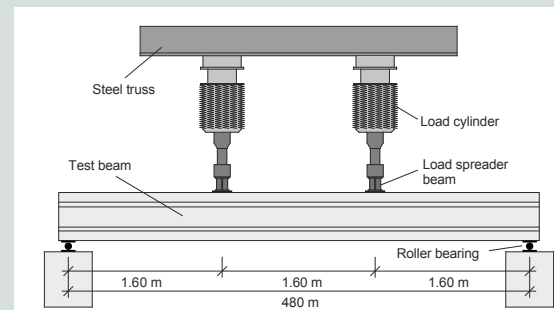
Experimental setup and procedure

Figure 5 shows the test setup, which was designed as a four-point bending test with a span of 4.80 m (15.75 ft) and load spacing of 1.60 m (5.25 ft). The test beams were simply supported on roller bearings on both ends to avoid constraining forces. The single loads were applied by two load cylinders driven by a hydraulic pulsator.

Initially, the beams were loaded twice monotonically to about 110% of the upper cyclic load level in approximately 10 kN (2.25 kip) load increments (Fig. 6). The initial static loading was used to crack all beams. Cracks were generated to consider the most unfavorable situation in terms of fretting actions at the strands and because cracking cannot be excluded even in prestressed concrete beams, for example, due to stresses above the fatigue loads (overloads). Then, the constant cyclic loading was applied with a frequency of 3 Hz (180 cycles per minute). At regular intervals of about 0.5 million load cycles, the cyclic loading was stopped and the beams were loaded monotonically to the upper cyclic load level to determine the time- and load-cycle-dependent load-deflection characteristics of the beams. In addition, beam B7 was loaded periodically to an overload of 120% of the upper cyclic load level. During cyclic testing, concrete and steel strains, crack widths, and beam deflections were continuously monitored with strain gauges and displacement transducers. In general, the measured crack widths proved to be clear indicators of broken wires in the prestressing strands. Nevertheless, acceleration sensors were also used to detect broken wires. All tests were conducted until total failure of the beams occurred.

Determination of cyclic loads, stress ranges, and fatigue load level

Table 2 shows the minimum cyclic loads $F_{fat,min}$, maximum cyclic loads $F_{fat,max}$, and resulting stress ranges $\Delta\sigma_p$ for each



Experimental test setup



Beam B7 after fatigue failure

Figure 5. Experimental setup. Note: 1 m = 3.281 ft.

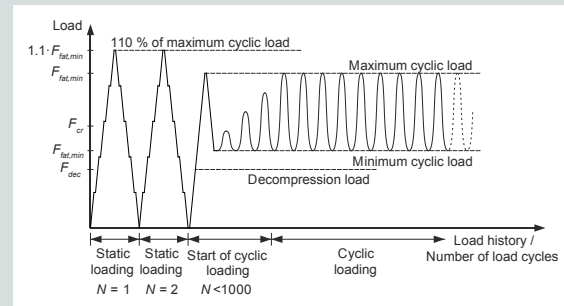


Figure 6. Test procedure. Note: F_{cr} = cracking load; F_{dec} = decompression load; $F_{fat,max}$ = maximum fatigue/cyclic load; $F_{fat,min}$ = minimum fatigue/cyclic load; N = number of load cycles.

beam, which were determined using theoretical section analyses using a linear-elastic stress-strain relationship for the concrete (without considering tensile strength) as well as for the reinforcing and prestressing steel. The moduli of elasticity were determined from compressive tests of concrete cylinders and tensile tests of steel samples (Table 1). The effective prestress level at the start of the test was determined by calculating the prestress losses according to EC2. Based on the initial static tests (first and second load cycles) (Fig. 6), the experimental cracking and decompression loads were determined and used to verify the theoretical calculations (Table 2).

Figure 7 compares the calculated concrete and steel strains with the experimental values measured by different strain

Table 2. Experimental and calculated cracking and decompression loads (per load cylinder) and calculated ultimate capacity and resulting fatigue load levels

Beam	Cracking load		Decompression load		Fatigue load		Calculated stress range $\Delta\sigma_{p,cal}$ MPa	Calculated ultimate capacity $F_{u,cal}$ kN	Fatigue load level	
	Experimental $F_{cr,exp}$ kN	Calculated $F_{cr,cal}$ kN	Experimental $F_{dec,exp}$ kN	Calculated $F_{dec,cal}$ kN	Minimum $F_{fat,min}$ kN	Maximum $F_{fat,max}$ kN			Minimum FLL_{min}	Maximum FLL_{max}
B5	88	85	69	64	94	122	143	212	0.44	0.58
B6	83	79	58	59	70	100	103	226	0.31	0.44
B7	80	78	60	58	70	100	105	225	0.31	0.44
B8	84	84	63	64	70	100	96	202	0.35	0.50
B9.1	83	83	63	63	80	95	61	200	0.40	0.48
B9.2	83	83	63	63	80	105	130	200	0.40	0.53
B10	84	81	56	61	75	95	79	204	0.37	0.47
B11	75	82	57	61	70	103	102	232	0.30	0.45
B12	84	83	58	62	70	97	99	190	0.37	0.51
B13	81	80	54	60	70	95	74	220	0.32	0.43

Note: 1 kN = 0.225 kip; 1 MPa = 0.145 ksi.

gauges during the initial static beam B7 test. Figure 7 shows the strain distribution considering the dead load at time of prestressing $F_{dead,0}$, as well as the strain distribution at time of testing under cracking load F_{cr} and minimum $F_{fat,min}$ and maximum cyclic load level $F_{fat,max}$. In addition, Fig. 7 shows the experimental and calculated load-strain relationship for concrete, reinforcing steel, and prestressing strands. These diagrams demonstrate that the calculated concrete and steel strains correlate very well with the measured experimental values.

Besides the stress ranges in the strands, the maximum fatigue load level FLL_{max} was used to evaluate the fatigue life of the beams. The maximum fatigue load level was calculated by the ratio of the maximum cyclic load $F_{fat,max}$ and the ultimate capacity of the beam $F_{u,cal}$, which corresponds to the ratio of the maximum fatigue moment to the ultimate moment capacity $M_{fat,max} / M_{u,cal}$. The ultimate capacity was determined by cross-sectional analysis using the experimental stress-strain relationship of concrete, reinforcing steel, and strands from the compressive tests of concrete cylinders and tensile tests of steel samples. Table 2 gives the calculated ultimate capacity as well as the resulting minimum fatigue load level FLL_{min} and maximum fatigue load level FLL_{max} . The calculated maximum fatigue load level of the beams was between 43% and 58% of ultimate capacity.

Fatigue test results

Deflection and cracking

The flexural behavior of pretensioned concrete beams under cyclic loading was characterized by an increase in deflec-

tions and crack widths during cyclic loading. In general, the midspan deflection of the beams increased with increasing cycles. However, when all tests are compared, a clear and uniform relationship between midspan deflection and the total number of load cycles is not identifiable (Fig. 8), considering also that the beam B9 test was stopped before failure after about 22 million load cycles (B9.1) and later continued at an increased cyclic load level until fatigue failure (B9.2).

To better compare the deflection behavior of different tests, Fig. 8 shows the beam deflection at maximum fatigue load in relation to the deflection of the cracked beam in the second cycle δ_2 as a function of relative number of load cycles N/N_{tot} , where N is the number of load cycles and N_{tot} is the total number of load cycles until beam failure. As previous studies have shown (for example, Abeles et al.,¹¹ Slepetz,¹² Harajli and Naaman,¹⁴ Overman et al.,¹⁵ and Hagenberger¹⁹), the deflection curve can be divided into the following three typical phases, depending on the relative number of load cycles:

- In the early stage of cyclic loading (phase I), deformations increase significantly due to redistribution of concrete and steel stresses caused by cyclic creep and change of stiffness in concrete.
- In phase II, deformations gradually increase at a low rate.
- In phase III, at about 80% of the number of load cycles before total failure of the beam, the deflections (and crack widths) increase rapidly caused by progressive failure of individual wires.

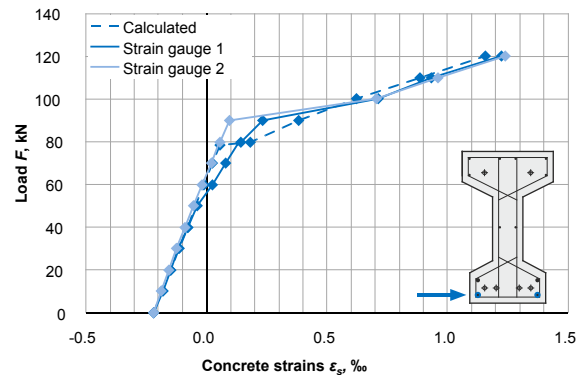
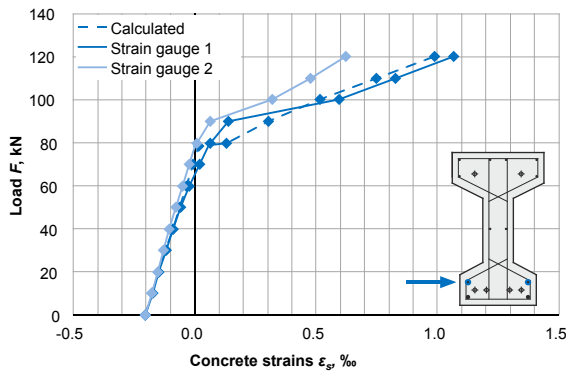
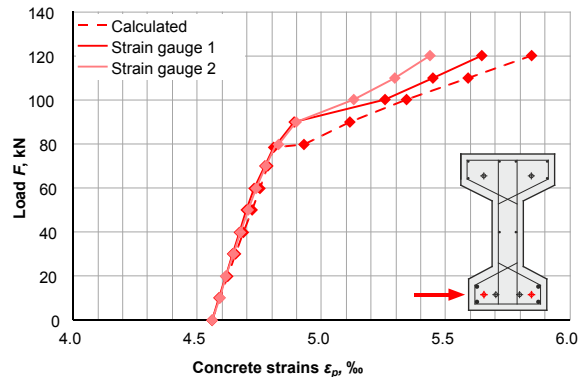
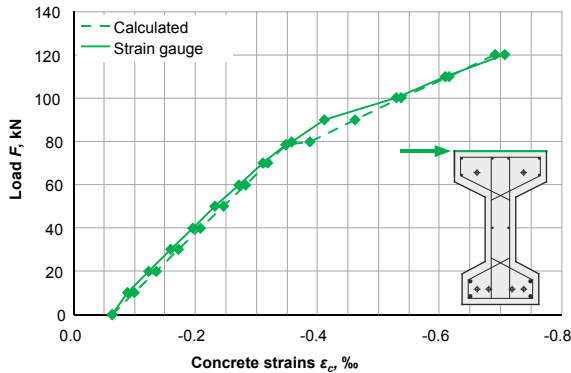
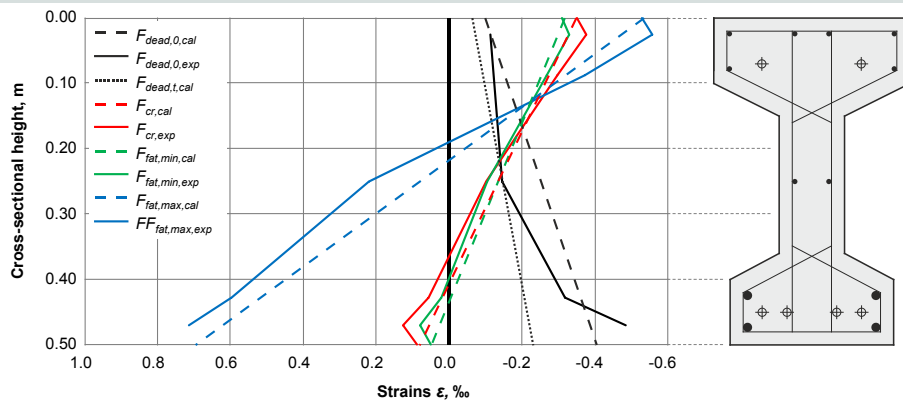


Figure 7. Experimental and calculated load-strain relationships of beam B7 for the first load cycle. Note: $F_{cr,cal}$ = calculated cracking load; $F_{cr,exp}$ = experimental cracking load; $F_{dead,t,cal}$ = calculated dead load of the beam at beginning of test including prestress losses; $F_{dead,0,cal}$ = calculated dead load of the beam at time of prestressing without time-dependent prestress losses; $F_{dead,0,exp}$ = experimental dead load of the beam at time of prestressing without time-dependent prestress losses; $F_{fat,max,cal}$ = calculated maximum fatigue/cyclic load; $F_{fat,max,exp}$ = experimental maximum fatigue/cyclic load; $F_{fat,min,cal}$ = calculated minimum fatigue/cyclic load; $F_{fat,min,exp}$ = experimental minimum fatigue/cyclic load. 1 kN = 0.225 kip; 1 m = 3.281 ft.

The flexural cracks in the middle of the beams were well distributed, with an average crack spacing of about 75 to 150 mm (3 to 6 in.), which corresponds to the stirrup spacing of 75 mm (3 in.). **Figure 9** shows the crack patterns of beams B6 and B7. The crack widths on the beams in the first and second load cycles were less than 0.05 mm (0.002 in.) at minimum fatigue load $F_{fat,min}$ and less than 0.10 mm (0.004 in.) at maximum fatigue load $F_{fat,max}$. The increase in crack width as the number of load cycles increases is similar to the three-phase deflection behavior. In contrast to the deflection and crack width, the crack depth remained nearly constant or propagated at a low rate during cyclic loading. After the first

wire breaks, at about 80% of the total number of load cycles, the crack depth propagated quickly into the top flange of the beams and finally expanded in different directions just before total failure (**Fig. 10**).

Fatigue failure

All test specimens failed in the beam area with constant moment and at a location where a concrete crack propagated into the top flange of the beams (**Fig. 9** and **10**). **Table 3** gives the number of load cycles at which fatigue failure of the first N_1 , second N_2 , and third wire N_3 occurred. Failure of the first three wires corre-

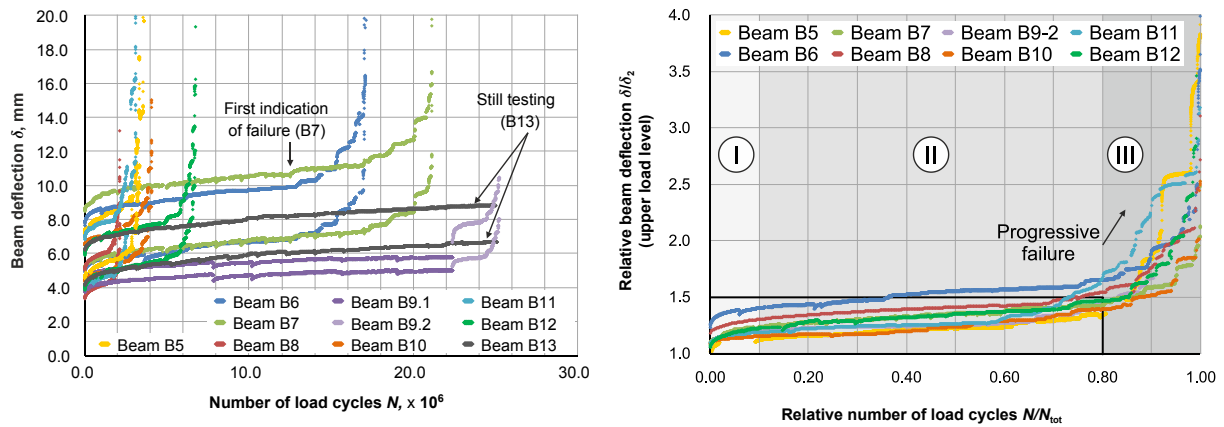


Figure 8. Deflection behavior of the beams. Note: I = phase I of cyclic loading; II = phase II of cyclic loading; III = phase III of cyclic loading; N = number of load cycles; N_{tot} = total number of load cycles (until beam failure); δ = midspan deflection; δ_2 = midspan deflection in second load cycle. 1 mm = 0.0394 in.

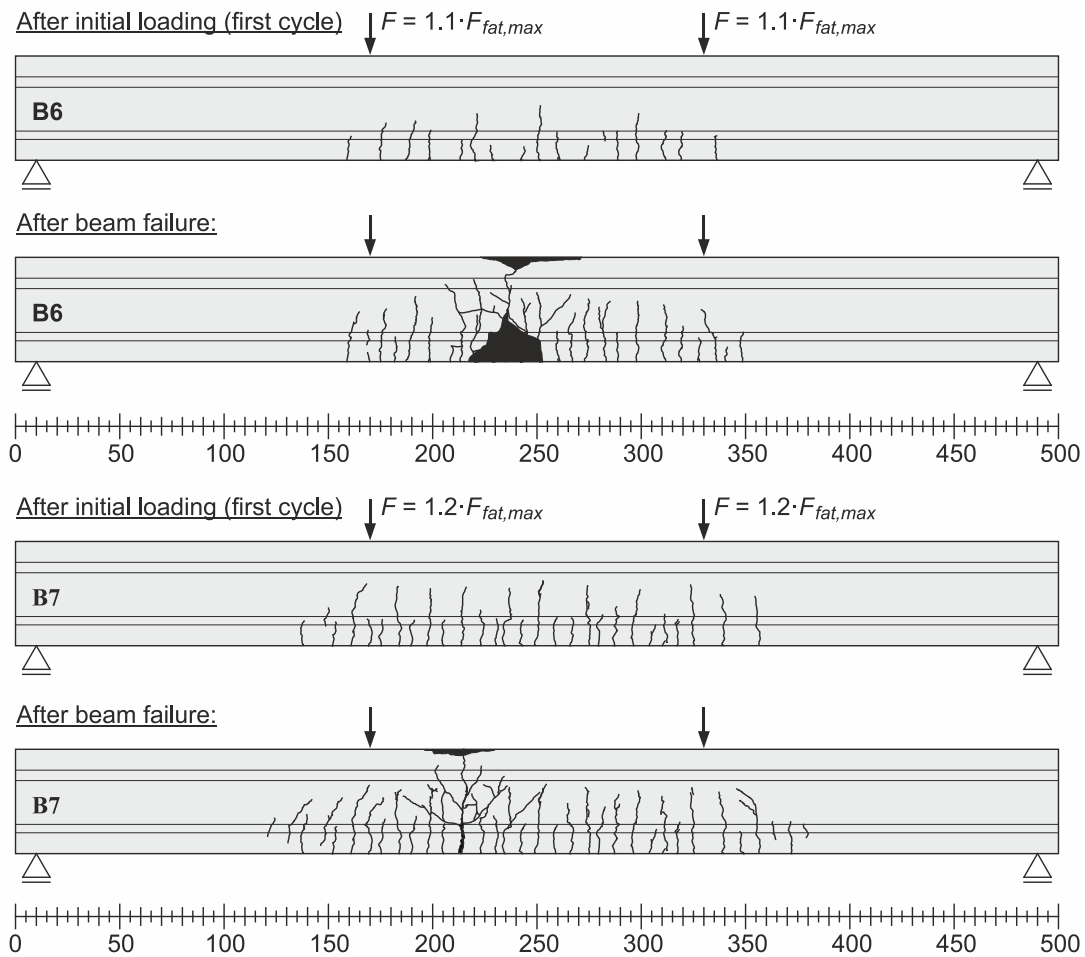


Figure 9. Crack pattern of beam B6 and B7 after first cycle and after beam failure. Note: Scale dimensions are in millimeters. F = applied load of the beam (per hydraulic cylinder); $F_{fat,max}$ = maximum fatigue/cyclic load. 1 mm = 0.0394 in.

Table 3. Number of load cycles until wire breaks and total beam failure

Beam	Number of load cycles				
	$N_1, \times 10^6$	$N_2, \times 10^6$	$N_3, \times 10^6$	$N_{tot}, \times 10^6$	N_1/N_{tot}
B5	2.226	2.731	3.106	3.618	0.62
B6	12.910	13.082	14.098	17.115	0.75
B7	12.538	12.732	16.984	21.162	0.59
B8	1.485	1.487	1.497	2.150	0.69
B9.1	n/a	n/a	n/a	22.401*	n/a
B9.2	1.719	1.856	1.987	2.868	0.60
B10	1.482	1.532	1.809	4.080	0.36
B11	1.781	1.822	1.833	3.116	0.57
B12	4.864	4.964	5.684	6.791	0.72
B13	still testing			25.000*	n/a

Note: N_{tot} = total number of load cycles until beam failure; N_1 = number of load cycles until first wire break; N_2 = number of load cycles until second wire break; N_3 = number of load cycles until third wire break; n/a = not applicable.

* No indication of damage

sponds to about a 10% reduction of the prestressing steel area. Table 3 also shows the number of cycles at which total fatigue failure of the beam occurred. The fatigue failure of the beams was initiated by the first wire break between 36% and 75% of the total number of load cycles (Table 3). Up to this point, the strand and reinforcement stresses and stress ranges indicated by the strain gauges remained roughly constant. The stresses and stress ranges in the strands then increased continuously due to the reduced strand area following each wire break, accelerating the fatigue damage to the beams. Finally, the total fatigue failure of the beams occurred after a significant number of wire breaks. The wire breaks were detected by sudden increases in crack width and deflection during the monitoring (Fig. 8). After testing, the strands were uncovered by removing the concrete (Fig. 11) and the wire breaks caused by fatigue were counted.

Fatigue life

To evaluate the fatigue life of the embedded prestressing strands, the stress ranges in the strands and the maximum fatigue load level were plotted against the number of cycles representing the fatigue life. The fatigue life was considered to be the number of load cycles at the first wire break because from this point the ultimate capacity under static loading is no longer ensured.

Figure 12 compares the fatigue life of the prestressing strands with previous fatigue tests of pretensioned concrete beams from the literature and the normative S-N curve and endurance limits, confirming a reduced fatigue life compared with normative specifications, such as similarly indicated in Fig. 1.

The fatigue life of beam B5, which was loaded with a relatively high strand stress range $\Delta\sigma_p$ of 143 MPa (20.7 ksi) and a

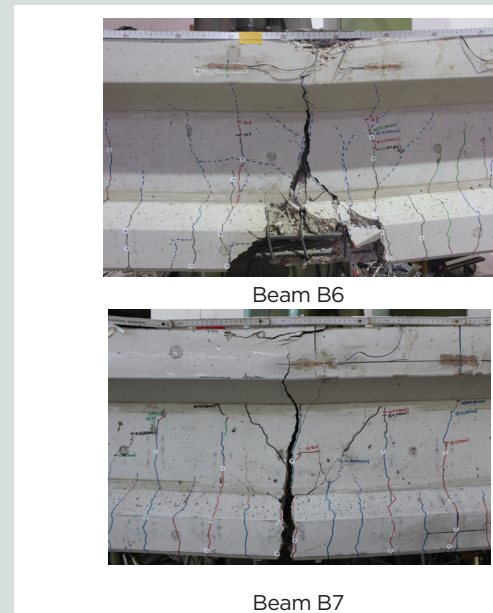


Figure 10. Failed section of beams B6 and B7.

fatigue load level of 58%, was comparable to previous fatigue test results from the literature with a similar stress range and load level. However, compared with the normative S-N curve according to EC2 and MC2010, the fatigue life of beam B5 was highly overestimated by a factor of about 10.

Although beam B7 was loaded with an overload of 120% of the upper cyclic load level every 0.5 million cycles, the first fatigue failure of a wire occurred at almost the same num-



Figure 11. Dismantling of strands in bottom flange of beam B7 after failure.

ber of load cycles (12.538×10^6) as beam B6 (12.910×10^6) with the same beam configuration and similar strand stress range. A reduced fatigue life caused by frequent overloads, mentioned by Harajli and Naaman,¹⁴ could not be confirmed. Compared with beams B6 and B7, beam B12, which had the same concrete (C50/60) and a similar strand stress range but less tensile reinforcement, failed after a reduced number of cycles (4.864×10^6). On one hand, the reduced fatigue life of beam B12 can be explained by a higher fatigue load level (51%) compared with beams B6 and B7 (both 44%) (**Fig. 13**). On the other hand, a smaller amount of tensile reinforcement results in reduced bond characteristics and a higher degradation of bond near concrete cracks. The reduction of fatigue life caused by the amount of tensile reinforcement was also observed in beam B8 (1.485×10^6) and B11 (1.781×10^6), which were constructed using high-strength C80/90 concrete.

Although the fatigue life of the high-strength concrete beams (B8 and B11) was much smaller than that of the normal-strength concrete beams (B6, B7, and B12), it is assumed that both the concrete strength and different concrete mixture

proportions (for example, the content of fines) influence the fatigue life of pretensioned concrete beams. This correlation has already been observed by the authors in tensile tests on single strands embedded in concrete as well as fatigue tests on post-tensioned concrete beams (B1 to B4).^{27,28}

Beams B9 and B10, both constructed using high-strength concrete and a small amount of tensile reinforcement (same configuration as beam B8), were tested with smaller strand stress ranges $\Delta\sigma_p$ of 61 MPa (8.8 ksi) and 79 MPa (11.5 ksi), respectively. The beam B9 test was stopped after 22.401×10^6 cycles (about 85 days of testing) with no indication of imminent fatigue failure (B9.1). The test was then continued (B9.2) with increased cyclic loading, resulting in a strand stress range $\Delta\sigma_p$ of 130 MPa (18.8 ksi). This caused the beam to fail after 1.719×10^6 cycles. Although the strand stress range of beam B10 was much smaller, no enhanced fatigue life (1.482×10^6 cycles) was observed.

Beam B13, constructed using normal-strength C50/60 concrete and more tensile reinforcement, achieved about 25×10^6

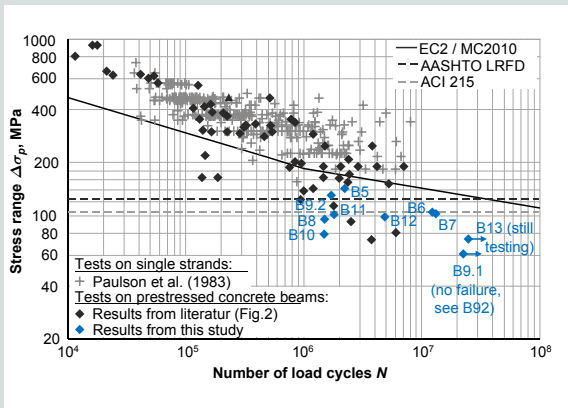


Figure 12. Fatigue test results of pretensioned concrete beams based on the stress range in prestressing steel. Note: AASHTO LRFD = American Association of State Highway and Transportation Officials' *AASHTO LRFD Bridge Design Specifications*; ACI 215 = the American Concrete Institute's *Considerations for the Design of Concrete Structures Subjected to Fatigue Loading* (ACI PRC-215-92); EC2/MC2010 = European Committee for Standardization's *Eurocode 2 or fib Model Code for Concrete Structures 2010*. 1 MPa = 0.145 ksi.

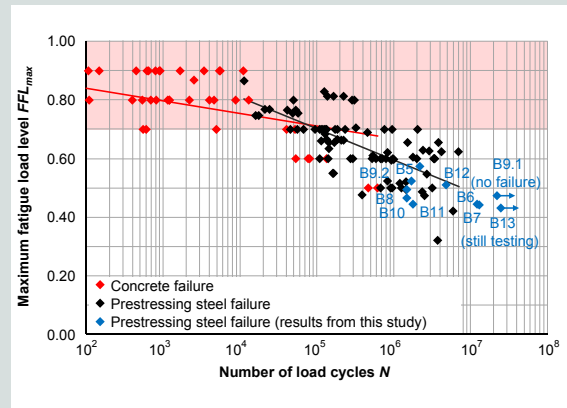


Figure 13. Fatigue test results of pretensioned concrete beams based on the fatigue load level. Note: Concrete failure = results from Venuti (1965) and Slepetz (1968); Prestressing steel failure = results from Ozell and Ardaman (1956); Nordby and Venuti (1957); Bate (1962); Warner and Hulsbos (1964); Venuti (1965); Abeles, Brown, and Hu (1974); Rabbat, Kaar, Russel, and Bruce (1979); Harajli and Naaman (1984); Overman, Breen, and Frank (1984); Muller and Dux (1992); and Rao and Frantz (1996).

load cycles with no indication of failure. This test will be continued up to at least 50×10^6 cycles to determine a possible fatigue endurance limit.

Overall, the fatigue tests showed that the fatigue life of pretensioned concrete beams is very sensitive to changes in the strand stress range and fatigue load level as well as to the concrete mixture proportions and the amount of tensile reinforcement.

Conclusion

Fatigue tests of pretensioned concrete beams from the literature indicate a reduced fatigue life compared with normative fatigue specifications. Because only a small number of high-cycle fatigue tests are available, a total of nine additional fatigue tests were conducted on pretensioned concrete beams for this study. These tests extended the data set of high-cycle fatigue test results for pretensioned concrete beams with load levels of about 50% and strand stress ranges $\Delta\sigma_p$ of about 100 MPa (14.5 ksi). In addition, the concrete mixture proportions and the amount of tensile reinforcement were varied within these tests. Based on the presented fatigue tests, the following conclusions can be drawn:

- The maximum fatigue load level and the cyclic steel stress range can be considered the main variables to describe the fatigue failure and fatigue life of pretensioned concrete beams.
- Irrespective of the various influencing parameters, the correlation between steel stress range (or fatigue load level) and the fatigue life of pretensioned concrete beams continues in the long-life region at least up to a stress

range $\Delta\sigma_p$ of approximately 100 MPa (14.5 ksi). Thus, the S-N curve according to EC2 and MC2010, as well as the endurance limits recommended by the AASHTO LRFD specifications and ACI PRC-215, do not thoroughly reflect the presented test results with stress ranges $\Delta\sigma_p$ of about 100 MPa. As a result, further considerations are required to derive a feasible fatigue model that provides an enhanced and safe estimation of the fatigue life of pretensioned concrete beams at low stress ranges and high numbers of load cycles.

- With respect to the influence of tensile reinforcement, the test results suggest that the fatigue life of pretensioned concrete beams is improved by an increase in tensile reinforcement.
- A significant influence of the concrete mixture proportions on the fatigue life of the beams was observed. This is assumed to be more related to the concrete ingredients (for example, the content of fines and the type of coarse aggregate) than to the concrete strength.
- The flexural fatigue behavior of pretensioned concrete beams can be specified by a typical deflection curve with an increasing number of load cycles. The fatigue failure of the beam is indicated by a rapid increase in deflections at about 80% of the number of load cycles before total failure of the beam, which is caused by progressive failure of individual wires of the strands.

Acknowledgments

The investigations presented in this paper were conducted at the iBMB Division of Concrete Construction of the Tech-

nische Universität Braunschweig within a research project funded by the Deutsche Forschungsgemeinschaft (German Research Foundation) project 351987113. The authors acknowledge this financial support. The authors also gratefully acknowledge Rekers Betonwerk GmbH & Co. KG for producing the beams.

References

1. CEN (European Committee for Standardization) Technical Committee CEN/TC250. 2004. *Eurocode 2: Design of Concrete Structures – Part 1-1: General Rules and Rules for Buildings*. EN 1992-1-1. Brussels, Belgium: CEN.
2. fib (Fédération Internationale du Béton). 2013. *fib Model Code for Concrete Structures 2010*. Berlin, Germany: Ernst & Sohn.
3. AASHTO (American Association of State Highway and Transportation Officials). 2014. *AASHTO LRFDF Bridge Design Specifications*. 7th ed. Washington, DC: AASHTO.
4. ACI (American Concrete Institute) Committee 215. 1992. *Considerations for the Design of Concrete Structures Subjected to Fatigue Loading*. ACI PRC-215-92. Farmington Hills, MI: ACI.
5. Ozell, A. M., and E. Ardaman. 1956. “Fatigue Tests of Pre-tensioned Prestressed Beams.” *Journal of the American Concrete Institute* 53 (10): 413–424.
6. Nordby, G. M., and W. J. Venuti. 1957. “Fatigue and Static Tests of Steel Strand Prestressed Beams of Expanded Shale Concrete and Conventional Concrete.” *Journal of the American Concrete Institute* 54 (8): 141–160.
7. Ozell, A. M., and J. F. Diniz. 1958. “Fatigue Tests of Prestressed Concrete Beams Pretensioned with ½ inch Strands.” *PCI Journal* 3 (1): 79–88.
8. Bate, S. C. C. 1962. “An Experimental Study of Strand in Prestressed Concrete Beams under Static and Repeated Loading.” *Proceedings of the Institution of Civil Engineers* 23 (4): 625–638.
9. Warner, R. F., and C. L. Hulsbos. 1964. *Probable Fatigue Life of Prestressed Concrete Beams Part I–IV*. Report 223.24C1-4, Lehigh University, Bethlehem, PA.
10. Venuti, W. J. 1965. “A Statistical Approach to the Analysis of Fatigue Failure of Prestressed Concrete Beams.” *Journal of the American Concrete Institute* 62 (11): 1375–1394.
11. Abeles, P. W., E. I. Brown II, and C. H. Hu. 1974. “Fatigue Resistance of Under-reinforced Prestressed Beams Subjected to Different Stress Ranges; Miner’s Hypothesis.” ACI Special Publication SP41-11: 237–277.
12. Slepetz, J. M. 1968. “Behavior of Rectangular Prestressed Concrete Beams Subjected to Heavy Repeated Loads.” PhD diss., Duke University, Durham, NC.
13. Rabbat, B. G., P. H. Kaar, H. G. Russel, R. N. Bruce Jr. 1979. “Fatigue Tests of Pretensioned Girders with Blanketed and Draped Strands.” *PCI Journal* 24 (4): 88–114.
14. Harajli, M. H., and A. E. Naaman. 1984. “Deformation and Cracking of Partially Prestressed Concrete Beams under Static and Cyclic Fatigue Loading.” Report UMEE 84R1. Ann Arbor, MI: College of Engineering, University of Michigan.
15. Overman, T. R., J. E. Breen, and K. H. Frank. 1984. *Fatigue Behavior of Pretensioned Concrete Girders*. Report 300-2F. Austin, TX: Center for Transportation Research, University of Texas at Austin.
16. Bökamp, H. 1991. “Ein Beitrag zur Spannstahlermüdung unter Reibdauerbeanspruchung bei Teilweiser Vorspannung.” PhD diss., RWTH Aachen, Germany.
17. Muller, J. F., and P. F. Dux. 1992. *Fatigue of Prestressed Concrete Beams with Inclined Strands*. Report CE 135. Brisbane, Australia: Department of Civil Engineering, University of Queensland.
18. Rao, C., and G. C. Frantz. 1996. “Fatigue Tests of 27-Year-Old Prestressed Concrete Bridge Box Beams.” *PCI Journal* 41 (5): 74–83.
19. Hagenberger, M. J. 2004. “Consideration of Strand Fatigue for Load Rating Prestressed Concrete Bridges.” PhD diss., University of Texas at Austin.
20. Heller, B. E. 2003. “Fatigue Response of Pretensioned Concrete Beams.” MS thesis, University of Texas at Austin.
21. Grunert, J. P. 2006. “Zum Tragverhalten von Spannbetonfertigteiltalbalken aus Stahlfaserbeton ohne Betonstahlbewehrung.” PhD diss., TU Braunschweig, Germany.
22. Empelmann, M., and C. Sender. 2010. “Sachstandbericht zur Dauerschwingfestigkeit von Spannstählen unter Dynamischer Beanspruchung im Eingebauten Zustand.” Bauforschung Band T 3245. Stuttgart: Fraunhofer IRB.
23. Maurer, R., G. Heeke, H. Kiziltan, A. Kolodziejczyk, K. Zilch, D. Dunkelberg, and B. Fitik. 2012. “Nachrechnung von Betonbrücken zur Bewertung der Tragfähigkeit Bestehender Bauwerke.” Report from Bundesanstalt für Straßenwesen B89.
24. Paulson Jr., C., K. H. Frank, and J. E. Breen. 1983. *A Fatigue Study of Prestressing Strand*. Report 300-1. Austin, TX: Center for Transportation Research, University of Texas at Austin.

25. Edwards, A. D., and A. Picard. 1972. "Fatigue Characteristics of Prestressing Strand." *Proceedings of the Institution of Civil Engineers* 53 (2): 323–336.
26. Remitz, J., and M. Empelmann. 2018. "Specific Influences on Fatigue Life of Prestressing Steel." In *Proceedings of 12th Japanese German Bridge Symposium, September 2018, Munich, Germany*.
27. Remitz, J., and M. Empelmann. 2020. "Cyclic Tensile Tests on Prestressing Strands Embedded in Concrete." *Materials and Structures* 53 (3). DOI: 10.1617/s11527-020-01484-x.
28. Remitz, J., and M. Empelmann. 2015. "Ermüdungsfestigkeit von Eingebauten Spanngliedern—Versuche an Spannbetontträgern." *Bauingenieur* 90 (12): 553–561.

Notation

- A_p = cross-sectional area of prestressing strands
- A_s = cross-sectional area of reinforcing steel
- E_{cm} = average concrete modulus of elasticity based on three cylinders tested
- $f_{ctm,sp}$ = average concrete splitting tensile strength based on three cylinders tested
- F = load applied to the beam per hydraulic cylinder
- F_{cr} = cracking load
- $F_{cr,cal}$ = calculated cracking load
- $F_{cr,exp}$ = experimental cracking load
- $F_{dead,t,cal}$ = calculated dead load of the beam at beginning of test including prestress losses
- $F_{dead,0}$ = dead load of the beam at time of prestressing without time-dependent prestress losses
- $F_{dead,0,cal}$ = calculated dead load of the beam at time of prestressing without time-dependent prestress losses
- $F_{dead,0,exp}$ = experimental dead load of the beam at time of prestressing without time-dependent prestress losses
- F_{dec} = decompression load
- $F_{dec,cal}$ = calculated decompression load
- $F_{dec,exp}$ = experimental decompression load
- $F_{fat,max}$ = maximum fatigue/cyclic load

- $F_{fat,max,cal}$ = calculated maximum fatigue/cyclic load
- $F_{fat,max,exp}$ = experimental maximum fatigue/cyclic load
- $F_{fat,min}$ = minimum fatigue/cyclic load
- $F_{fat,min,cal}$ = calculated minimum fatigue/cyclic load
- $F_{fat,min,exp}$ = experimental minimum fatigue/cyclic load
- F_u = ultimate load capacity
- $F_{u,cal}$ = calculated ultimate load capacity
- FFL_{max} = maximum fatigue load level
- FFL_{min} = minimum fatigue load level
- $M_{fat,max}$ = maximum fatigue/cyclic moment
- M_u = ultimate moment capacity
- N = number of load cycles
- N_{tot} = total number of load cycles until beam failure
- N_1 = number of load cycles until first wire break
- N_2 = number of load cycles until second wire break
- N_3 = number of load cycles until third wire break
- δ = midspan deflection of the beams
- δ_2 = midspan deflection of the beams in second load cycle
- $\Delta\sigma_p$ = cyclic stress range in the prestressing steel/strands
- ϵ = strain in the beam cross section
- ϵ_c = concrete strain
- ϵ_p = strain in the prestressing strands
- ϵ_s = strain in the mild reinforcing steel
- $\sigma_p^{(0)}$ = initial prestressing steel/strand stress
- $\sigma_{p,t}$ = prestressing steel/strand stress at start of test (including prestress losses)

About the authors



Jörn Remitz, MSc, is a research assistant in the Institute of Building Materials, Concrete Construction and Fire Protection, Division of Concrete Construction at Technische Universität (TU) Braunschweig, Germany.



Martin Empelmann, EngD, is a professor in the Institute of Building Materials, Concrete Construction and Fire Protection, Division of Concrete Construction at TU Braunschweig, as well as scientific director of the Civil

Engineering Materials Testing Institute Braunschweig. His research focuses on all aspects of the construction, design, maintenance, and retrofit of plain, reinforced, and prestressed concrete structures. He is actively involved in various associations and committees that work, for example, on guidelines and standards such as *Eurocode 2*. He is also an independent checking engineer for structural design.

Abstract

Prestensioned concrete beams are widely used as bridge girders for simply supported bridges. Understanding the fatigue behavior of such beams is very important for design and construction to prevent fatigue failure. The fatigue behavior of prestensioned concrete beams is mainly influenced by the fatigue of the prestressing strands. The evaluation of previous test results from the literature indicated a reduced fatigue life in the long-life region compared with current design methods and specifications. Therefore, nine additional high-cycle fatigue tests were conducted on prestensioned concrete beams with strand stress ranges of about 100 MPa (14.5 ksi). The test results confirmed that current design methods and specifications overestimate the fatigue life of embedded strands in prestensioned concrete beams.

<https://doi.org/10.15554/pcij67.1-02>

Keywords

Cyclic loading, fatigue, prestressed concrete beam, prestressing strand, S-N curve.

Review policy

This paper was reviewed in accordance with the Precast/Prestressed Concrete Institute's peer-review process.

Reader comments

Please address any reader comments to *PCI Journal* editor-in-chief Tom Klemens at tklemens@pci.org or Precast/Prestressed Concrete Institute, c/o *PCI Journal*, 8770 W. Bryn Mawr Ave., Suite 1150, Chicago, IL 60631. [1](#)